Article

Journal of
Nanoscience and Nanotechnology
Vol. 17, 4247–4250, 2017
www.aspbs.com/jnn

Electric-Field Induced Abrupt and Multi-Step Insulator-Metal Transitions in Vanadium Dioxide Nanobeams

Servin Rathi[1], Inyeal Lee[1], Jeong Min Baik[2], and Gil-Ho Kim[1,*]

[1] *School of Electronic and Electrical Engineering and Sungkyunkwan Advanced Institute of Nanotechnology (SAINT), Sungkyunkwan University, Suwon 16419, Korea*
[2] *School of Mechanical and Advanced Materials Engineering, Ulsan National Institute of Science and Technology (UNIST), Ulsan 689-805, Korea*

Both abrupt and multi-step Insulator-metal transitions triggered by applied voltage (electric field) were observed in VO_2 nanobeams. The multi-step transition occurs due to nucleation and subsequent expansion of multiple insulating and metallic domains across the nanobeam whereas the abrupt transition results from the propagation of a parallel metallic domain across the nanobeam. A simple power dissipation based model was also used to study the local temperature evolution during these transitions in the nanobeam. Both types of transitions are suitable for prospective application in resistive memory and switches.

Keywords: Insulator-Metal Transitions, Domains, Vanadium Dioxide Nanobeams, Joule-Heating.

1. INTRODUCTION

Vanadium dioxide (VO_2), a strongly correlated-metal oxide, has been studied extensively for the transition in its electronic and lattice properties across insulator-metal transitions (IMT).[1,2] The dimerization of V^{4+} leads to localization of $3d^1$ electrons on V sites in a spin singlet states, thus an insulating state due to coulombic repulsion results in the opening up of a band gap (≈0.6 eV) via splitting of *d* orbitals.[3,4] Various studies have indicated transition based on both critical electron (Motts) and phonon densities (Peierls transition) based theories, however an exact mechanism is still debatable.[5] The transition from insulating to metallic states and vice-versa can be triggered by various stimuli like thermal, electric-filed, doping, strain, electrostatic charge accumulation, etc.[2,6,7] The transition temperature from the insulating to the metallic phase for VO_2 is closest to room temperature (67 °C) among other oxides, with a switching time on the order of pico-sec, which makes it desirable for potential technological applications including switches, sensors and memristors.[8–12] Normally, IMT is an abrupt transition marked by a change of several order of resistance across the transition temperature and presided by the formation of mixed metal and insulating domains which plays a critical role in the transition.[13,14] When the size of device becomes comparable to the size of these electronic domains, in the range of around 100 nm, then the electronic properties of individual domains can be studied through electronic measurements as multiple step transition instead of a typical single-step abrupt transition.[15] In such devices, the role of these electronic domains in inducing physical transitions can be studied through multi-step transition in both VO_2 thin-films and nanowires from the viewpoint of the fundamental physics of spatially inhomogeneous domain systems and for applications in multi-bit resistive memory which store multiple bits per element and switching.[16] Although, in previous studies the evolution and propagation of electronic domains both with thermal and voltage stimuli has been studied, however, a well-defined voltage induced multi-step transitions was missing, which set the platform for the current study.[15] Here, we have observed and discussed both abrupt and multi-step transitions induced and mediated through domains by applied voltage or electric field in the VO_2 nanobeam based devices.

*Author to whom correspondence should be addressed.

2. MATERIALS AND METHODS

The VO_2 NBs used in the experiment were grown using the vapor transport technique from the VO_2 powder source.[12] Figure 1 shows the Raman spectrum and scanning electron microscopic images of the VO_2 NB device. Normally, the NB with width and thickness in the range of 50–300 nm were used to fabricate the devices. The NBs displayed a near-rectangular cross-section, as seen from the Figure 1(d), and a good aspect-ratio of 2:1. The device fabrication can be broadly divided in two steps, firstly, the as-grown VO_2 NBs were detached from the original SiO_2 substrate by ultra-sonication for a few seconds. Then, with a micropipette, the suspension of NBs in IPA solution was dispersed onto a clean 300 nm SiO_2/*n*-type Si substrate. After the solution dried out, it was rinsed in IPA followed by cleaning with N_2 gun. This method is not only helpful in selecting longer nanowires for fabricating devices, but also reduces the substrate interaction effects, as the transferred VO_2 NBs interact weakly with the under-lying substrate as compared to the as-grown NBs.[9] Thereafter, the selected NBs were contacted using typical UV photolithography, which was followed by an *e*-beam deposition of Ti/Au (10/150 nm) electrodes and finally lift-off in acetone (to remove the photoresist layer) results in the pattern as seen in Figure 1(b). Further, a rapid thermal annealing at 200 °C for 1 minute was also carried out in an argon environment to establish good ohmic contacts. Figure 1(a) shows the characteristic Raman spectrum of a VO_2 NB recorded at room temperature. The peaks in the VO_2 NB's spectra are identified at 197($\boldsymbol{A_g}$), 227($\boldsymbol{A_g}$), 264($\boldsymbol{B_g}$), 311($\boldsymbol{B_g}$), 343($\boldsymbol{B_g}$), 396($\boldsymbol{A_g}$), 443($\boldsymbol{B_g}$), 614($\boldsymbol{A_g}$) cm^{-1}, which correspond to V–V and V–O lattice motion and bonding in the NB. These Raman-active modes are the clear signature of the monoclinic (M1) phase and are found to be consistent with previously reported measurement on VO_2 NBs.[9,17]

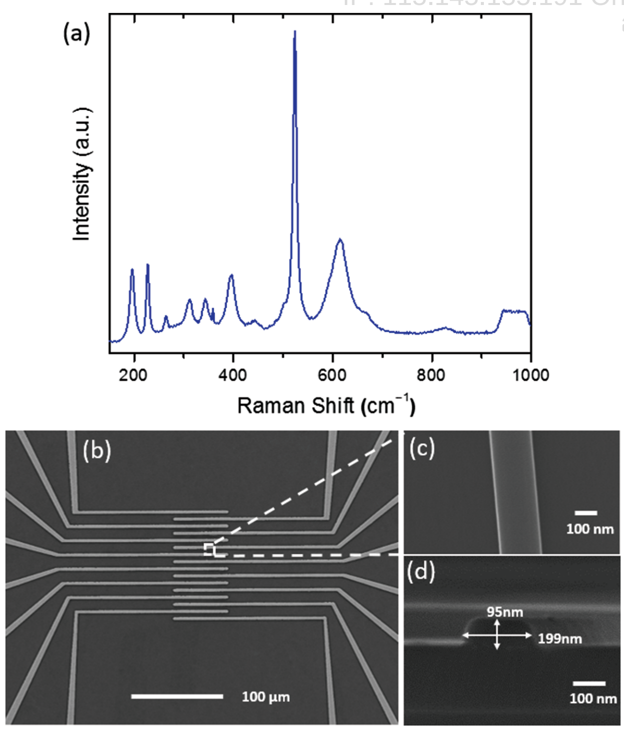

Figure 1. (a) Raman spectrum of the monoclinic phase of VO_2 NB, (b–c) Scanning Electron Microscopic (SEM) image of the patterned VO_2 NB and a higher magnification image, (d) shows a near-rectangular cross-section of a synthesized NB observed from the side-edge of the SiO_2/Si substrate.

3. RESULTS AND DISCUSSION

Figure 2(a) shows the schematic of the fabricated device and measurement set-up to record current–voltage (*I–V*) characteristics, where Keithley 4200 SCS system was used to measure *I–V* characteristics with the sample mounted on a variable temperature hot-chuck system (MS-Tech Corp.). Figure 2(b) shows *I–V* curve obtained at room-temperature and ambient conditions, where the straight line shows good ohmic contacts. Usually, for a fixed gap between the electrodes, the current or resistance of a NB depends upon various factors like the aspect-ratio of the NBs and defects in the NBs, which are generally related to the oxygen deficiency related defects such as oxygen vacancies, interstitials or lattice defects. Such defects not only serve as source of electrons but may also act as nucleation sites for the first order phase transitions. The density of these defects depends on various factors during the growth conditions and device fabrication steps.[8]

Figure 2(c) shows a typical dual sweep *I–V* behaviour of a device, from 0 to +5 V and back, measured at 50 °C. The *I–V* curve shows abrupt transition from insulator to metal state at a threshold voltage (V_{IMT}) of 3.8 V, whereas a reverse metal to insulator transition occurs at 2.4 V, (V_{MIT}). As seen from the figure, these transition appears to be abrupt and sharp, indicating a seeding and simultaneous extension of one or more parallel metallic domain along the NB (as shown in the inset of Fig. 2(c)) in the electric filed direction due to the nano-confinement effect in the NBs.[14] Usually, such metallic domain in NB covers the entire cross-section due to high aspect-ratio (length/width) of the NBs, whereas, the observed hysteresis has its origin in the retention of metallic properties by the metallic domains fractions. These hysteretic voltage-triggered transitions are associated with complex mechanism, where both structural and electrical properties of the VO_2 undergoes through series of transitions. The schematics in the inset of Figure 2(c) illustrate the transition in the lattice from tetragonal to monoclinic and vice-versa, via dimerization and tilting of vanadium chains which simultaneously leads to localization of $3d^1$ electrons and splitting of the orbital, thus creating a small band gap of 0.6 eV, as illustrated in the inset of Figure 3(a). Various intertwined factors like thermal, electric field, Joule-heating etc., play

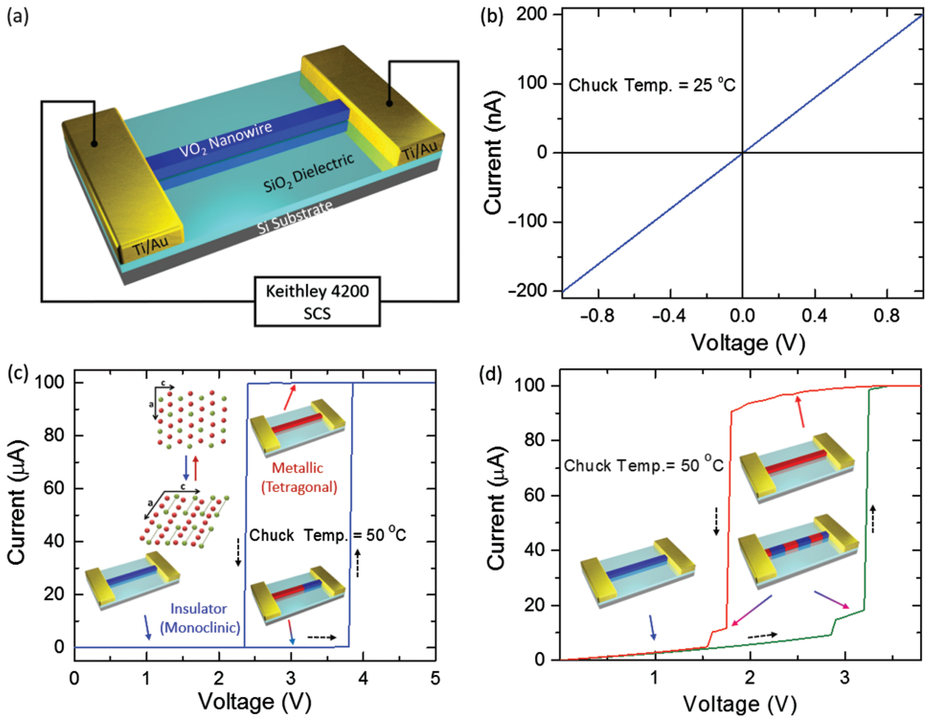

Figure 2. (a) Schematic of the fabricated NB device with Ti/Au electrodes and electrical biasing for measurement with Keithley 4200 SCS, (b) *I–V* measurement of a VO_2 NB device at room-temperature. (c) Dual sweep *I–V* curve showing the abrupt insulator-metal transition in the VO_2 NB device with the voltage sweep at an ambient temperature of 50 °C. The inset shows lattice arrangement in metallic and insulating phases, (d) Dual sweep *I–V* curve showing muti-step transitions, with the device schematics in the Figures (c and d) insets show the domains mediated insulator-metal transition in the VO_2 NB device.

crucial role in such transition and as the lattice- and energy band based electronic properties are interwoven, therefore the exact mechanism responsible for the observed hysteretic voltage or thermal based transitions are still debatable.

However, a different kind of transition is observed in Figure 2(d), where the transition appears in steps, in contrast to the one observed in Figure 2(c). Such multi-step transition was also observed in the reverse sweep as well. In the previous studies, such multi-step transitions in thin-films and nanowires were explained in terms of series and parallel metallic domains propagation. The abrupt transition as observed above can be explained by the parallel domains propagation whereas in the case multi-step transitions, where the phase transformations from insulating to metallic occurs via nucleation and expansion of individual metallic domains, which are isolated from each other by insulating domains, as illustrated in the inset

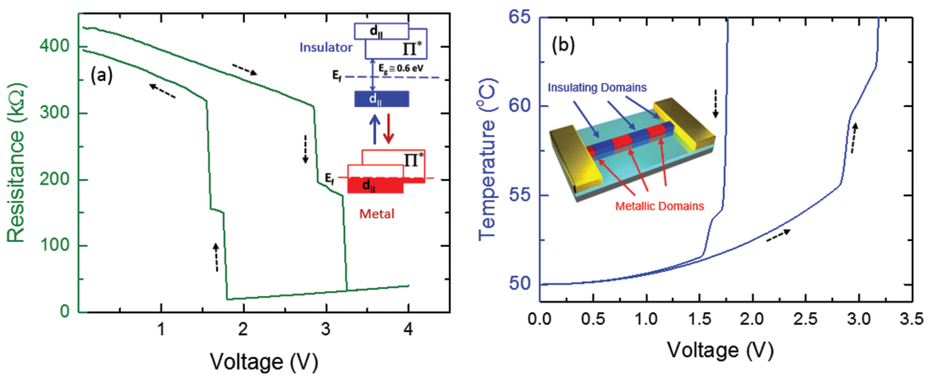

Figure 3. (a) Resistance plot with voltage sweep, with the inset showing schematics of energy band diagram in insulating and metallic phases, (b) the plot of VO_2 NB temperature with voltage sweep as obtained from the first-order theoretical fitting, showing the step heating and cooling of the NB during the transition phase.

of Figure 2(d). Therefore, the multi-step transition arises either due to the expansion of such metallic domains or transition of insulating domain to metallic, with the final abrupt-step transition occurring with the transition of the last bottleneck insulating domain to metallic domain, as observed in Figure 2(d). The number of steps, their width and position cannot be reliably predicted as it depends critically on number of factors like crystallinity, stoichiometry, distribution and activation of interstitial impurities/defect density, and interface stresses in VO_2 with an underlying substrate and these factors also determine the nucleation of metallic domains under the applied stimuli.[15]

The voltage induced transition observed in the NB can also be studied by using a simple power dissipation model. Considering an instantaneous equilibrium with the environment and for negligible ohmic contact resistance, we have derived temperature dependence with voltage and current in the device, as follows;[9]

$$T = T_0 + V^2/kR \quad \text{or} \quad T = T_0 + IV/k \tag{1}$$

where k is a collection of thermal parameters, including the thermal coefficient and heat capacity of the NB and the underlying substrate surface, V, I and R are the voltage, current and resistance across the NB, respectively, and T and T_0 are the temperature of NB and ambient environment, respectively.

Figure 3(a) plots the resistance versus voltage curve with the inset showing the energy band diagram for both insulating and metallic phases based on the molecular orbital and crystal field theory employed by Goodenough, where the d_{ll} band (whose orbitals are directed towards the next vanadium ions (V^{4+}) along the rutile c-axis and are therefore characteristic features of V^{4+}–V^{4+} interaction) splits as VO_2 undergoes a transition from metal to an insulating state.[2] The steps in both upward and downward sweep can be seen clearly and are identical to that of resistance versus temperature curves,[15] underlying the fact that the local temperature in the NB scale linearly with Joule-heating. The plot in Figure 4(b) is obtained by using Eq. (1) and it shows that the variation in temperature is gradual before and after the transitions, whereas it is very steep at the transition points, which can be linked to the Joule-Heating-induced temperature rise at the transition of insulating to metallic domains and vice-versa. The predicated temperature of 62 °C and 54 °C for upward and downward sweep also agrees well with the other published results.[8]

4. CONCLUSION

The two different type of insulator metal transition, abrupt and multi-step, has been studied in the VO_2 NBs. These transitions were observed by applying voltage across the NB and the temperature rise with applied voltage was deduced based on a first order Joule-heating model. The abrupt transition was explained through the concept of a parallel domain formation, whereas the series metallic domains explained the multi-step transitions. Besides pure aspects of VO_2 research, such multi-step transitions can be used for prospective device applications like memristors, resistive switches, sensors and multi-bit resistive memories.

Acknowledgments: This research was supported by Basic Science Research Program through the National Research Foundation of Korea (NRF) funded by the Ministry of Education, Science and Technology (2013R1A2A2A01069023 and 2015H1D3A1062519).

References and Notes

1. M. Imada, A. Fujimori, and Y. Tokura, *Rev. Mod. Phys.* 70, 1039 (**1998**).
2. Z. Yang, C. Ko, and S. Ramanathan, *Annu. Rev. Mater. Res.* 41, 337 (**2011**).
3. M. Nakano, K. Shibuya, D. Okuyama, T. Hatano, S. Ono, M. Kawasaki, Y. Iwasa, and Y. Tokura, *Nature* 487, 459 (**2012**).
4. T. L. Cocker, L. V. Titova, S. Fourmaux, G. Holloway, H.-C. Bandulet, D. Brassard, J.-C. Kieffer, M. A. E. Khakani, and F. A. Hegmann, *Phys. Rev. B* 85, 155120 (**2012**).
5. V. Eyert, *Phys. Rev. Lett.* 107, 016401 (**2011**).
6. A. Zimmers, L. Aigouy, M. Mortier, A. Sharoni, S. Wang, K. G. West, J. G. Ramirez, and I. K. Schuller, *Phys. Rev. Lett.* 110, 056601 (**2013**).
7. C. Ko and S. Ramanathan, *Appl. Phys. Lett.* 93, 252101 (**2008**).
8. S. Rathi, J.-H. Park, I. Lee, M. J. Kim, J. M. Baik, and G.-H. Kim, *Appl. Phys. Lett.* 103, 203114 (**2013**).
9. S. Rathi, J.-H. Park, I. Lee, J. M. Baik, K. S. Yi, and G.-H. Kim, *J. Phys. D. Appl. Phys.* 47, 295101 (**2014**).
10. N. Manca, L. Pellegrino, T. Kanki, S. Yamasaki, H. Tanaka, A. S. Siri, and D. Marré, *Adv. Mater.* 25, 6430 (**2013**).
11. S. Rathi, I. Y. Lee, J. H. Park, B. J. Kim, H. T. Kim, and G. H. Kim, *ACS Appl. Mater. Interfaces* 6, 19718 (**2014**).
12. J. M. Baik, M. H. Kim, C. Larson, C. T. Yavuz, G. D. Stucky, A. M. Wodtke, and M. Moskovits, *Nano Lett.* 9, 3980 (**2009**).
13. T. Kanki, K. Kawatani, H. Takami, and H. Tanaka, *Appl. Phys. Lett.* 101, 1 (**2012**).
14. H. Ueda, T. Kanki, and H. Tanaka, *Appl. Phys. Lett.* 102, 2011 (**2013**).
15. H. Takami, T. Kanki, and H. Tanaka, *Appl. Phys. Lett.* 104, 1 (**2014**).
16. J. Wei, Z. Wang, W. Chen, and D. H. Cobden, *Nat. Nanotechnol.* 4, 1 (**2009**).
17. H.-T. Kim, B.-G. Chae, D.-H. Youn, G. Kim, K.-Y. Kang, S.-J. Lee, K. Kim, and Y.-S. Lim, *Appl. Phys. Lett.* 86, 242101 (**2005**).

Received: 7 June 2016. Accepted: 25 June 2016.